TMPRSS2:ERG Fusion-Associated Deletions Provide Insight into the Heterogeneity of Prostate Cancer

Sven Perner,[1,2,4] Francesca Demichelis,[1,2,6] Rameen Beroukhim,[2,3,7] Folke H. Schmidt,[1,2] Juan-Miguel Mosquera,[1,2] Sunita Setlur,[1,2] Joelle Tchinda,[1,2] Scott A. Tomlins,[8] Matthias D. Hofer,[1,2] Kenneth G. Pienta,[9,10] Rainer Kuefer,[5] Robert Vessella,[11] Xiao-Wei Sun,[1,2] Matthew Meyerson,[2,3,7] Charles Lee,[1,2] William R. Sellers,[2,3,7] Arul M. Chinnaiyan,[8,9] and Mark A. Rubin[1,2,3]

[1]Department of Pathology, Brigham and Women's Hospital; [2]Harvard Medical School; [3]Dana-Farber Cancer Institute, Boston, Massachusetts; [4]Department of Pathology, University of Ulm; [5]Department of Urology, University Hospital Ulm, Ulm, Germany; [6]Bioinformatics Group, SRA Division, ITC-irst, Trento, Italy; [7]Broad Institute of Harvard and Massachusetts Institute of Technology, Cambridge, Massachusetts; Departments of [8]Pathology, [9]Urology, and [10]Medical Oncology, University of Michigan, Ann Arbor, Michigan; and [11]University of Washington, Seattle, Washington

Abstract

Prostate cancer is a common and clinically heterogeneous disease with marked variability in progression. The recent identification of gene fusions of the 5′-untranslated region of TMPRSS2 (21q22.3) with the ETS transcription factor family members, either ERG (21q22.2), ETV1 (7p21.2), or ETV4 (17q21), suggests a mechanism for overexpression of the ETS genes in the majority of prostate cancers. In the current study using fluorescence in situ hybridization (FISH), we identified the TMPRSS2:ERG rearrangements in 49.2% of 118 primary prostate cancers and 41.2% of 18 hormone-naive lymph node metastases. The FISH assay detected intronic deletions between ERG and TMPRSS2 resulting in TMPRSS2:ERG fusion in 60.3% (35 of 58) of the primary TMPRSS2:ERG prostate cancers and 42.9% (3 of 7) of the TMPRSS2:ERG hormone-naive lymph node metastases. A significant association was observed between TMPRSS2:ERG rearranged tumors through deletions and higher tumor stage and the presence of metastatic disease involving pelvic lymph nodes. Using 100K oligonucleotide single nucleotide polymorphism arrays, a homogeneous deletion site between ERG and TMPRSS2 on chromosome 21q22.2-3 was identified with two distinct subclasses distinguished by the start point of the deletion at either 38.765 or 38.911 Mb. This study confirms that TMPRSS2:ERG is fused in approximately half of the prostate cancers through deletion of genomic DNA between ERG and TMPRSS2. The deletion as cause of TMPRSS2:ERG fusion is associated with clinical features for prostate cancer progression compared with tumors that lack the TMPRSS2:ERG rearrangement. (Cancer Res 2006; 66(17): 8337-41)

Introduction

Prostate cancer is a common and clinically heterogeneous disease with marked variability in progression. The recent identification of gene fusions of the 5′-untranslated region (UTR) of TMPRSS2 (21q22.3) with the ETS transcription factor family members, either ERG (21q22.2), ETV1 (7p21.2; ref. 1), or ETV4 (17q21; ref. 2), provides a mechanism for overexpression of ETS genes in prostate cancer. TMPRSS2 is highly expressed in prostate cancer and contains androgen response elements in the promoter (3). Recent work showed that exposure to androgen regulates the fused ETS family member. We observed that in the TMPRSS2:ERG positive prostate cancer cell line VCap (4) exposure to a synthetic androgen specifically increased ERG expression, whereas no change in expression was observed in the TMPRSS2:ERG-negative LNCaP prostate cancer cell line.

Therefore, the gene fusion identified in prostate cancer represents a new paradigm for epithelial tumors, which have until now been characterized only by nonspecific chromosomal aberrations. Hematologic malignancies and sarcomas are often characterized by balanced, disease-specific chromosomal rearrangements (i.e., balanced translocations). The prototypic example is the malignant transformation of WBC to chronic myeloid leukemia (CML) through a translocation between chromosomes 9 and 22 (Philadelphia chromosome) resulting in the novel tyrosine kinase fusion protein, BCR-ABL. Understanding the molecular and clinical diversity of CML came when it was discovered that, in addition to the bcr-abl translocation, a subset of CML cases harbor a deletion of the derivative chromosome 9 involved in the reciprocal translocation, which is associated with poor clinical outcome (5, 6).

In the current study, we report the presence of common intronic deletions on chromosome 21q22.2-3 as cause of the TMPRSS2:ERG fusion and associations with disease progression. This report presents insight as to how the presence of genomic deletions in the TMPRSS2:ERG rearrangement in prostate cancer may account for molecular and clinical heterogeneity.

Materials and Methods

Clinical samples. Clinically localized prostate cancer samples and hormone-refractory samples were collected as part of institutional review board–approved research protocols at the University of Ulm (7) and University of Michigan (8), respectively. All samples were reviewed by one pathologist for uniform grading.

Fluorescence in situ hybridization (FISH) experiments were conducted on two prostate cancer tissue microarrays composed of 897 tissue cores from 211 patients. This cohort represents men with both clinically localized and clinically advanced prostate cancer as shown by the high pretreatment prostate-specific antigen (PSA) levels and high percentage of men with

Table 1. Clinical and pathologic demographics of 118 men with clinically localized prostate cancer treated by radical prostatectomy

	Count (*n*)	Column (%)
Age		
Less than or equal to the median	55	50.0
More than the median	55	50.0
Preoperative PSA (ng/mL)		
≤4	6	8.2
>4 and <10	13	17.8
≥10	54	74.0
Gleason score sum		
<7	7	6.0
7	51	43.6
>7	59	50.4
Nuclear grade		
1	—	—
2	38	35.5
3	69	64.5
Pathology stage (pT)		
pT$_2$	26	22.2
pT$_{3a}$	34	29.1
pT$_{3b}$	57	48.7
Surgical margins status		
Negative	30	27.8
Positive	78	72.2
Lymph node status (pN)		
N$_0$	52	44.1
N$_1$	56	47.5
N$_2$	10	8.5
PSA recurrence		
No	34	48.6
Yes	36	51.4

NOTE: Not all data points were available for all 118 cases.

metastases to pelvic lymph nodes (7). The patient demographics are presented in Table 1.

Cell lines and xenografts. Androgen-independent (PC-3, DU-145, HPV10, and 22Rvl) and androgen-sensitive (LNCaP) prostate cancer cell lines were purchased from the American Type Culture Collection (Manassas, VA) and maintained in their defined medium. HPV10 was derived from cells from a high-grade prostate cancer (Gleason score 4 + 4 = 8; ref. 9). 22Rv1 is a human prostate cancer epithelial cell line derived from a xenograft that was serially propagated in mice after castration-induced regression and relapse of the parental, androgen-dependent CWR22 xenograft (10). The VCaP cell line was derived from a vertebral metastatic lesion (4).

LuCaP 23.1, 35, 73, 77, 81, 86.2, 92.1, and 105 were derived from patients with androgen-independent hormone-refractory prostate cancer. LuCaP 49 and 115 are from patients with androgen-dependent prostate cancer. LuCaP 58 is derived from an untreated patient with metastatic disease and LuCaP 96 was from a hormone-refractory prostate cancer (11, 12). LuCaP 49 and 93 are hormone-insensitive (androgen receptor–negative) small cell prostate cancers with a neuroendocrine phenotype. LuCaP 23.1 is maintained in severe combined immunodeficient mice, and other xenografts are maintained by implanting tumors in male BALB/c *nu/nu* mice.

Determining *TMPRSS2:ERG* fusion status using dual-color interphase FISH. We have described previously the FISH analysis for the translocation of *TMPRSS2:ERG* (1). This break-apart assay is presented in Fig. 1 and Supplementary Fig. S1. For analyzing the *ERG* rearrangement on

chromosome 21q22.2, a break-apart probe system was applied, consisting of the biotin-14-dCTP-labeled BAC clone RP11-24A11 (eventually conjugated to produce a red signal) and the digoxigenin-dUTP-labeled BAC clone RP11-137J13 (eventually conjugated to produce a green signal), spanning the neighboring centromeric and telomeric regions of the *ERG* locus, respectively. All BAC clones were obtained from the BACPAC Resource Center (CHORI, Oakland, CA). Before tissue analysis, the integrity and purity of all probes were verified by hybridization to normal peripheral lymphocyte metaphase spreads. Tissue hybridization, washing, and fluorescence detection were done as described previously (13). One hundred eighteen cases of clinically localized prostate cancer, including 15 cases with corresponding hormone-naive metastatic lymph node samples, could be evaluated. Ninety-three cases could not be evaluated because of missing tissue on the tissue microarray (*n* = 54) or assay failure (*n* = 39).

The samples were analyzed under a ×60 oil immersion objective using an Olympus (Center Valley, PA) BX-51 fluorescence microscope equipped with appropriate filters, a charge-coupled device camera, and the CytoVision FISH imaging and capturing software (Applied Imaging, San Jose, CA). Evaluation of the tests was independently done by two pathologists (S.P. and J-M.M.). At least 100 nuclei per case were evaluated. Differences were refereed by a third pathologist (M.A.R.).

Oligonucleotide single nucleotide polymorphism array analysis. Single nucleotide polymorphism (SNP) detection on the 100K array began with a reduction in genome representation. Two aliquots of 250 ng genomic DNA were digested separately with *Xba*I/*Hin*dIII. The digested fragments were independently ligated to an oligonucleotide linker. The resulting products were amplified using a single PCR primer under conditions in
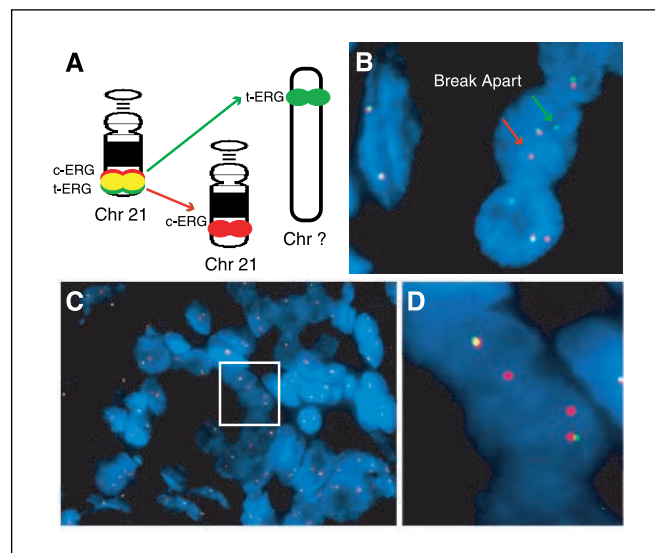

Figure 1. *A* to *D, TMPRSS2:ERG* gene fusion analysis by FISH. *A,* ideogram depicting the break-apart assay for the indirect detection of *TMPRSS2:ERG* fusion. Probes were designed against *ERG* locus showing the fluorochrome-labeled region telomeric (BAC clone RP11-137J13, green signal) and centromeric (BAC clone RP11-24A11, red signal) of the *ERG* locus on 21q22.3. The telomeric probe is distal to the one originally reported by Tomlins et al. (1). This set of probes appears yellow due to the overlap of the red centromeric and green telomeric probe in the nontranslocated allele. If a break occurs between the two probes, each color can be separately detected indirectly supporting the *TMPRSS2:ERG* gene fusion. *B,* interphase nuclei of a stromal cell (*left*) and a prostate cancer gland (*right*). The stromal cell is negative for fusion, confirmed by the presence of two juxtaposed red and green signals resulting in two yellow signals. The fusion in the prostate cancer gland nuclei results in the break apart of the yellow signal of one allele to generate distinct red and green signals (*arrows*; magnification, ×100 oil immersion objective). *C,* interphase nuclei of prostate cancer glands showing break apart and simultaneous deletion shown by loss of the telomeric (green-labeled) probe (magnification, ×100 oil immersion objective). *D,* magnified view of boxed area in (*C*) showing two nuclei with break apart and loss of the telomeric probe (magnification, ×60 oil immersion objective).

which 200- to 2,000-bp PCR fragments were amplified. The derived amplified pools of DNA were then labeled, fragmented further, and hybridized to separate *Hin*dIII and *Xba*I oligonucleotide SNP arrays. Arrays were scanned with a GeneChip Scanner 3000. Genotyping calls and signal quantification were obtained with GeneChip Operating System 1.1.1 and Affymetrix Genotyping Tools 2.0 software. Only arrays with genotyping call rates exceeding 90% were analyzed further. Raw data files were preprocessed and visualized in dChipSNP (14). In particular, preprocessing included array data normalization to a baseline array using a set of invariant probes and subsequent processing to obtain single intensity values for each SNP on each sample using a model-based (PM/MM) method (15).

Quantitative PCR for *TMPRSS2:ERG* and *TMPRSS2:ETV1* fusion transcripts. Quantitative PCR was done using SYBR Green dye (Qiagen, Valencia, CA) on a DNA engine Opticon 2 machine (MJ Research, Ramsey, MN). Total RNA was reverse transcribed into cDNA using Taqman reverse transcription reagents (Applied Biosystems, Foster City, CA) in the presence of random hexamers. All quantitative PCRs were done with SYBR Green Master Mix (Qiagen). We used primers that were described by Tomlins et al. (1) and are specific for the fusion (*TMPRSS2:ERG* forward TAGGCGC-GAGCTAAGCAGGAG and reverse GTAGGCACACTCAAACAACGACTGG and *TMPRSS2:ETV1* forward CGCGAGCTAAGCAGGAGGC and reverse CAGGCCATGAAAAGCCAAACTT). Glyceraldehyde-3-phosphate dehydrogenase (GAPDH) primers were described previously (16). Forward and reverse primers (10 μmol) were used and procedures were done according to the manufacturer's recommended thermocycling conditions. Threshold levels were set during the exponential phase of the quantitative PCR using Opticon Monitor analysis software version 2.02. The amount of each target gene relative to the housekeeping gene GAPDH for each sample was determined using the comparative threshold cycle method (Applied Biosystems User Bulletin 2). All reactions were subjected to melt curve analysis and products from selected experiments were resolved by electrophoreses on 2% agarose gel.

Statistics. The clinical and pathology variables were explored for associations with rearrangement status and with the presence of the deletion. χ^2 test and Fisher's exact test were used appropriately. Kaplan-Meier analysis was used to generate PSA recurrence-free survival curves of the pathology and the genomic alteration variables. Patients with prior neoadjuvant hormone ablation therapy were excluded. All statistics were done using SPSS 13.0 for Windows (SPSS, Inc., Chicago, IL) with a significance level of 0.05.

Results

To characterize the frequency of the *TMPRSS2:ERG* rearrangement in prostate cancer, we used a modified FISH assay from the assay described by Tomlins et al. (1). The original FISH assay used two probes located on *ERG* at the centromeric 3′ and telomeric
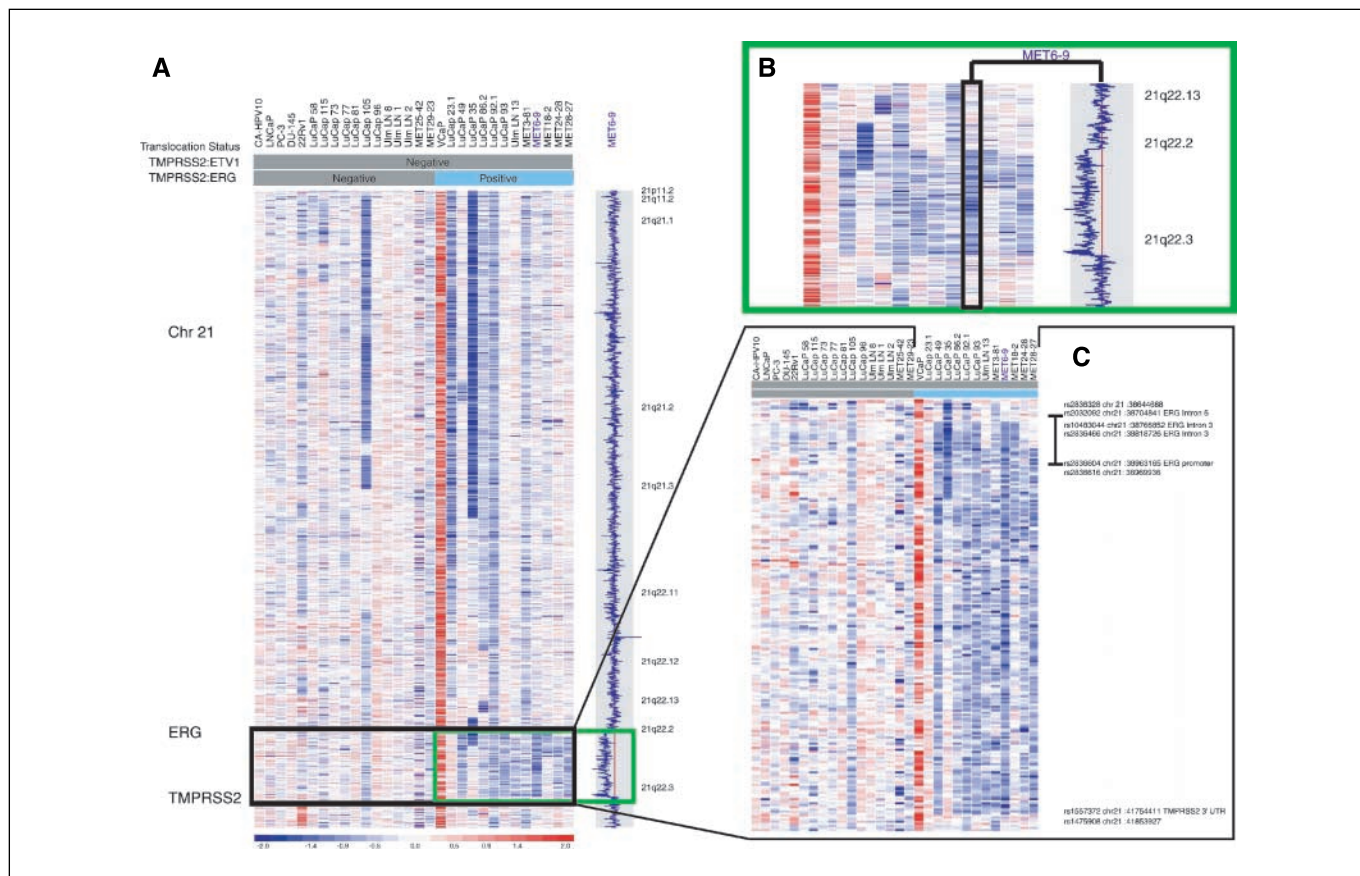

Figure 2. *A* to *C*, genomic deletions on chromosome 21 between *ERG* and *TMPRSS2*. Interrogating high-density 100K SNP arrays (∼110,000 loci on the genome) on a panel of 30 prostate cancer samples, we observed a commonly deleted area on chromosome 21q22.2-22.3, spanning the region between *ERG* and *TMPRSS2*. *A*, samples, including 6 cell lines, 13 xenografts, and 11 metastatic prostate cancer samples, were characterized for *TMPRSS2:ERG* and *TMPRSS2:ETV1* status (*gray columns*, negative status; *blue columns*, positive status) by quantitative PCR and/or FISH. *B*, magnification of the green framed box in (*A*). Signal intensity on the right is proportional to copy number intensity of a hormone-refractory metastatic prostate cancer sample (MET6-9). Interestingly, for *TMPRSS2:ERG* rearrangement-positive tumors, the 71% (5 of 7) hormone-refractory prostate cancer show a deletion between *TMPRSS2* and the *ERG* loci, whereas deletion was only identified in 1 of 4 hormone-naive metastatic prostate cancer samples (ULM LN 13). *C*, magnification of the black framed box in (*A*). SNP data include 25 loci along *ERG*, distributed from the gene promoter to intron 5 and 1 SNP on the 3′-UTR of *TMPRSS2*. There is significant homogeneity for the deletion borders with two subclasses distinguished by the start point of the deletion (either 38.765 or 38.911 Mb).
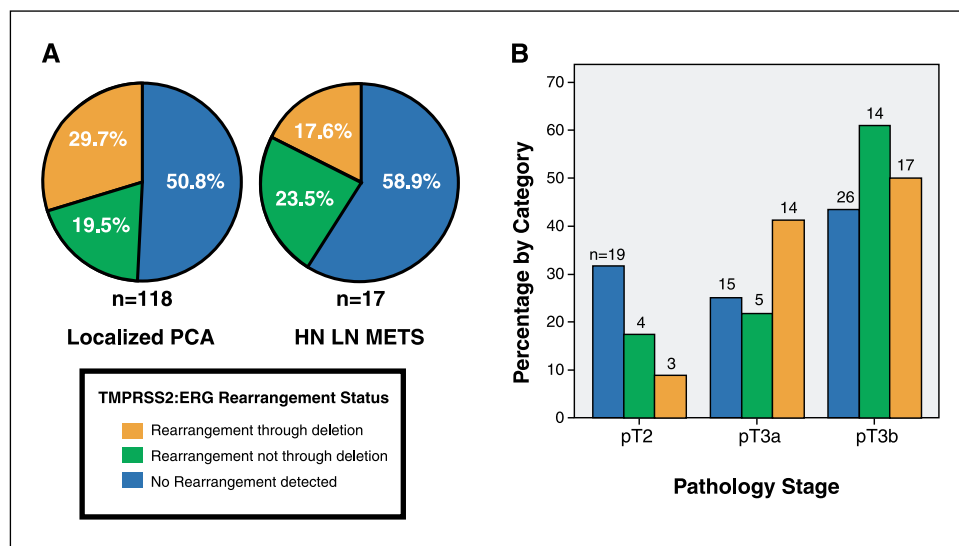
5′ ends. The new assay moved the 5′ probe in a telomeric direction (Supplementary Fig. S1). Using a prostate cancer screening tissue microarray, we observed that ∼70% of prostate cancer showing *TMPRSS2:ERG* rearrangement (Fig. 1*A* and *B*) also showed a loss of the green signal corresponding to the telomeric 5′ *ERG* probe (Fig. 1*C* and *D*), suggesting that this chromosomal region was deleted. We then used 100K oligonucleotide SNP arrays to characterize the extent of these deletions. By interrogating 30 prostate cancer samples, including cell lines, xenografts, and hormone-naive and hormone-refractory metastatic prostate cancer samples, we identified genomic loss between *ERG* and *TMPRSS2* on chromosome 21q23 (Fig. 2*A-C*). The rearrangement status for *TMPRSS2:ERG* and *TMPRSS2:ETV1* was determined for these 30 prostate cancer cases by FISH and/or quantitative PCR (Fig. 2*A*, *gray* and *light blue columns*). None of the samples tested showed a *TMPRSS2:ETV1* rearrangement. Discrete genomic loss was observed in *TMPRSS2:ERG* rearrangement-positive samples involving an area between *TMPRSS2* and the *ERG* loci for LuCaP 49, LuCaP 93, ULM LN 13, MET6-9, MET18-2, MET24-28, and MET28-27. The extent of these discrete deletions was heterogeneous. More extensive genomic loss on chromosome 21, including the area between *TMPRSS2* and the *ERG* loci, was observed in LuCaP 35, LuCaP 86.2, LuCaP 92.1, and MET3-81. The VCaP cell line and the xenograft LuCaP 23.1 did not show loss in this region. For a subset of samples, 45% (5 of 11) deletion occurs in proximity of *ERG* intron 3. For most samples, 64% (7 of 11) deletion ends in proximity of the SNP located on *TMPRSS2* (the next SNP in the telomeric direction is ∼100K bp distant). The VCaP cell line shows copy number gain along the entire chromosome 21. Interestingly, for *TMPRSS2:ERG* fused tumors, 71% (5 of 7) hormone-refractory prostate cancer cases show a deletion between *TMPRSS2* and the *ERG* loci, whereas the deletion was only identified in 25% (1 of 4) hormone-naive metastatic prostate cancer samples (ULM LN 13). There is significant homogeneity for the deletion borders with two distinct subclasses distinguished by the start point of the deletion (at either 38.765 or 38.911 Mb). None of the standard prostate cancer cell lines [PC-3, LNCaP, DU-145, or CWR22 (22Rv1)] showed the *TMPRSS2:ERG* or *TMPRSS2:ETV1* fusion. Several of the LuCaP xenografts show *TMPRSS2:ERG* fusion as result of the deletion, including LuCaP 49 (established from an omental mass) and LuCaP

93, both hormone-insensitive (androgen receptor–negative) small cell prostate cancers.

We also observed low-level copy number gain of *ERG* and *TMPRSS2* in a small subset of cases both with and without the *TMPRSS2:ERG* rearrangement (data not shown). The VCaP cell line derived from a hormone-refractory prostate cancer showed significant copy number gain on chromosome 21 (Fig. 2*A-C*), which was confirmed by FISH (data not shown).

To characterize the frequency and potential clinical significance of these observations, we examined 118 clinically localized prostate cancer cases by FISH. The clinical and pathology demographics are presented in Table 1. Using standard tissue sections from 10 cases that were represented on the tissue microarrays from this cohort, we observed the *TMPRSS2:ERG* rearrangement to be homogeneous for a given tumor. The *TMPRSS2:ERG* rearrangement was identified in 49.2% of the primary prostate cancer samples and 41.2% in the hormone-naive metastatic lymph node samples (Fig. 3*A*). Deletion of the telomeric probe (Fig. 1*C* and *D*, green signal) was observed in 60.3% (35 of 58) of the primary prostate cancer samples and 42.9% (3 of 7) of the hormone-naive lymph node tumors with *TMPRSS2:ERG* rearrangement. In the 15 cases where there was matched primary and hormone-naive lymph node tumors, there was 100% concordance for *TMPRSS2:ERG* rearrangement status, with 47% (7 of 15) of the pairs showing the rearrangement. Deletion of the telomeric (green signal) probe was concordantly seen in 42.9% (3 of 7) of the pairs. Interestingly, one primary prostate cancer and the matched hormone-naive metastatic sample showed randomly intermixed tumor cells where rearrangement without deletion was seen (see Supplementary Fig. S2).

We explored the associations between rearrangement status and clinical and pathologic variables (Fig. 3). *TMPRSS2:ERG* rearrangement through deletion was observed in a higher percentage of prostate cancer cases with high tumor stage (pT; $P = 0.03$; Fig. 3*B*) and metastases to pelvic lymph nodes (pN$_0$ versus pN$_{1-2}$; $P = 0.02$). We did not observe any significant associations between tumor grade (Gleason grade) and the *TMPRSS2:ERG* status. *TMPRSS2:ERG* rearranged prostate cancer through deletions showed a statistical trend for higher PSA biochemical recurrence when compared with nonfused prostate cancer.

Figure 3. *TMPRSS2:ERG* rearrangement in clinically localized prostate cancer and association with pathologic variables. *A, TMPRSS2:ERG* rearrangement was identified in 49.2% of the primary prostate cancer (*PCA*) samples and 41.2% in the hormone-naive metastatic lymph node samples (*HN LN METS*). Deletion of the telomeric probe (green signal) was observed in 60.3% (35 of 58) of the primary prostate cancer samples and 42.9% (3 of 7) of the hormone-naive lymph node tumors with *TMPRSS2:ERG* rearrangement. *B, TMPRSS2:ERG* rearranged tumors with deletions tended to be observed in a higher percentage of prostate cancer cases with advanced tumor stage ($P = 0.03$).

Discussion

The 42% *TMPRSS2:ERG* gene fusion identified in the current study is comparable with the 55% (16 of 29) reported by Tomlins et al. (1) and 78% (14 of 18) reported by Soller et al. (17). Intronic deletions located between *TMPRSS2* and *ERG* on chromosome 21q22.2-3 were observed in 60.3% of the *TMPRSS2:ERG* fusion-positive cases in the current study. The deletions appear in a consensus area but show variability within this area. The resolution of the 100K SNP array did not allow us to more precisely characterize the telomeric extent of these deletions in relationship to *TMPRSS2*. The FISH assay is an indirect test and therefore cannot directly confirm fusion of *TMPRSS2:ERG*. However, as we reported previously (1), 5′ RNA ligase-mediated rapid amplification of cDNA ends (RACE) analysis and sequencing of the reverse transcription-PCR (RT-PCR) product from 19 of 20 prostate cancer cases with ERG overexpression revealed a fusion of *TMPRSS2* with *ERG* by quantitative PCR and/or RACE. This shows that almost all prostate cancer samples with marked overexpression of ERG have a *TMPRSS2:ERG* rearrangement, and the overexpression occurs in about the same number of cases as the rearrangement. The current study identified significant associations with *TMPRSS2:ERG* gene fusion status and risk factors for disease progression. Petrovics et al. reported that high ERG expression is associated with better clinical outcome as determined by PSA biochemical failure (18). It is difficult to compare the results from the two studies as one evaluated ERG expression by RT-PCR in a PSA screened cohort and the current study evaluated *TMPRSS2:ERG* gene fusion status from a partially PSA screened high-risk European cohort. Future work will therefore focus on determining disease progression and risk based on the *TMPRSS2:ERG* rearrangement status and ERG expression in larger population-based cohorts using prostate cancer–specific survival as the end point.

By using Oncomine, a publicly available compendium of gene expression data, we were able to identify significantly down-regulated genes located in the area of the common deletion site. Loss of one or more of the genes located in the area of intronic loss may be associated with cancer progression in addition to the oncogenic potential of the *TMPRSS2:ERG* fusion product (Supplementary Fig. S3). For example, the loss of HMGN1 expression has been associated with tumor growth in cell line studies (19) and the underexpression of the ETS family member, Ets-2, has been associated with the reduction of antiapoptotic protein bcl-x(L) and growth regulatory factors cyclin D1 and c-myc in prostate cancer cell lines (20). The additional loss of these and other yet unidentified genes with tumor suppressor gene potential may explain the worse outcome compared with tumors with *TMPRSS2:ERG* fusion not through deletion. Ongoing work will examine the potential biological effect of *TMPRSS2:ERG* fusion mechanism on prostate cancer progression.

References

1. Tomlins SA, Rhodes DR, Perner S, et al. Recurrent fusion of TMPRSS2 and ETS transcription factor genes in prostate cancer. Science 2005;310:644–8.
2. Tomlins SA, Mehra R, Rhodes DR, et al. TMPRSS2:ETV4 gene fusions define a third molecular subtype of prostate cancer. Cancer Res 2006;66:3396–400.
3. Lin B, Ferguson C, White JT, et al. Prostate-localized and androgen-regulated expression of the membrane-bound serine protease TMPRSS2. Cancer Res 1999;59:4180–4.
4. Korenchuk S, Lehr JE, MClean L, et al. VCaP, a cell-based model system of human prostate cancer. In Vivo 2001;15:163–8.
5. Huntly BJ, Reid AG, Bench AJ, et al. Deletions of the derivative chromosome 9 occur at the time of the Philadelphia translocation and provide a powerful and independent prognostic indicator in chronic myeloid leukemia. Blood 2001;98:1732–8.
6. Sinclair PB, Nacheva EP, Leversha M, et al. Large deletions at the t(9;22) breakpoint are common and may identify a poor-prognosis subgroup of patients with chronic myeloid leukemia. Blood 2000;95:738–43.
7. Hofer MD, Kuefer R, Huang W, et al. Prognostic factors in lymph node-positive prostate cancer. Urology 2006;67:1016–21.
8. Shah RB, Mehra R, Chinnaiyan AM, et al. Androgen-independent prostate cancer is a heterogeneous group of diseases: lessons from a rapid autopsy program. Cancer Res 2004;64:9209–16.
9. Weijerman PC, Konig JJ, Wong ST, Niesters HG, Peehl DM. Lipofection-mediated immortalization of human prostatic epithelial cells of normal and malignant origin using human papillomavirus type 18 DNA. Cancer Res 1994;54:5579–83.
10. Sramkoski RM, Pretlow TG II, Giaconia JM, et al. A new human prostate carcinoma cell line, 22Rv1. In Vitro Cell Dev Biol Anim 1999;35:403–9.
11. Corey E, Quinn JE, Buhler KR, et al. LuCaP 35: a new model of prostate cancer progression to androgen independence. Prostate 2003;55:239–46.
12. Ellis WJ, Vessella RL, Buhler KR, et al. Characterization of a novel androgen-sensitive, prostate-specific antigen-producing prostatic carcinoma xenograft: LuCaP 23. Clin Cancer Res 1996;2:1039–48.
13. Rubin MA, Varambally S, Beroukhim R, et al. Overexpression, amplification, and androgen regulation of TPD52 in prostate cancer. Cancer Res 2004;64:3814–22.
14. Lin M, Wei LJ, Sellers WR, Lieberfarb M, Wong WH, Li C. dChipSNP: significance curve and clustering of SNP-array-based loss-of-heterozygosity data. Bioinformatics 2004;20:1233–40.
15. Li C, Wong WH. Model-based analysis of oligonucleotide arrays: expression index computation and outlier detection. Proc Natl Acad Sci U S A 2001;98:31–6.
16. Vandesompele J, De Preter K, Pattyn F, et al. Accurate normalization of real-time quantitative RT-PCR data by geometric averaging of multiple internal control genes. Genome Biol 2002;3:RESEARCH0034.
17. Soller MJ, Isaksson M, Elfving P, Soller W, Lundgren R, Panagopoulos I. Confirmation of the high frequency of the TMPRSS2/ERG fusion gene in prostate cancer. Genes Chromosomes Cancer 2006;45:717–9.
18. Petrovics G, Liu A, Shaheduzzaman S, et al. Frequent overexpression of ETS-related gene-1 (ERG1) in prostate transcriptome. Oncogene 2005;24:3847–52.
19. Birger Y, Catez F, Furusawa T, et al. Increased tumorigenicity and sensitivity to ionizing radiation upon loss of chromosomal protein HMGN1. Cancer Res 2005;65:6711–8.
20. Carbone GM, Napoli S, Valentini A, Cavalli F, Watson DK, Catapano CV. Triplex DNA-mediated downregulation of Ets2 expression results in growth inhibition and apoptosis in human prostate cancer cells. Nucleic Acids Res 2004;32:4358–67.

TMPRSS2:ERG Fusion-Associated Deletions Provide Insight into the Heterogeneity of Prostate Cancer

Sven Perner, Francesca Demichelis, Rameen Beroukhim, et al.

Updated version	Access the most recent version of this article at: http://cancerres.aacrjournals.org/content/66/17/8337
Supplementary Material	Access the most recent supplemental material at: http://cancerres.aacrjournals.org/content/suppl/2006/09/08/66.17.8337.DC1

Cited articles	This article cites 20 articles, 11 of which you can access for free at: http://cancerres.aacrjournals.org/content/66/17/8337.full#ref-list-1
Citing articles	This article has been cited by 59 HighWire-hosted articles. Access the articles at: http://cancerres.aacrjournals.org/content/66/17/8337.full#related-urls

E-mail alerts	Sign up to receive free email-alerts related to this article or journal.
Reprints and Subscriptions	To order reprints of this article or to subscribe to the journal, contact the AACR Publications Department at pubs@aacr.org.
Permissions	To request permission to re-use all or part of this article, use this link http://cancerres.aacrjournals.org/content/66/17/8337. Click on "Request Permissions" which will take you to the Copyright Clearance Center's (CCC) Rightslink site.